Dynamical inverse problem on a metric tree

Article *in* Inverse Problems · June 2011

DOI: 10.1088/0266-5611/27/7/075011

CITATIONS
8

READS
43

3 authors, including:

Sergei A. Avdonin
University of Alaska Fairbanks
115 PUBLICATIONS **1,338** CITATIONS
SEE PROFILE

Boris Belinskiy
University of Tennessee at Chattanooga
87 PUBLICATIONS **361** CITATIONS
SEE PROFILE

Dynamical Inverse Problem on a Metric Tree

S A Avdonin[1]‡, B P Belinskiy[2]§ and J V Matthews[2]‖

[1] University of Alaska Fairbanks, Fairbanks, AK 99775-6660, USA

[2] University of Tennessee at Chattanooga, 615 McCallie Avenue, Chattanooga, TN 37403-2598, USA

E-mail: s.avdonin@alaska.edu, Boris-Belinskiy@utc.edu, Matt-Matthews@utc.edu

Abstract. We consider the problem of reconstruction of the potential for the wave equation on a specific star graph using the dynamical Dirichlet-to-Neumann map. Our algorithm is based on the Boundary Control method. We reduce the problem of reconstruction to a second kind Fredholm integral equation, the kernel and the right-hand-side of which arise from an auxiliary second kind Volterra integral equation. A second-order accurate numerical method for the equations is described and implemented. Then several numerical examples demonstrate that the algorithm works and can be used to reconstruct an unknown potential accurately.

PACS numbers: 02.30.Zz, 02.10.Ox, 43.20.Tb, 02.30.Rz, 02.30.Jr, 02.30.Hq, 02.60.-x

AMS classification scheme numbers: 35R30, 34A55, 81U40, 35L10, 45D05, 65R20

Keywords: wave equation, boundary control method, inverse problem, Volterra equation, numerical analysis, noise

Submitted to: *Inverse Problems*

1. Introduction.

Initial boundary value problems (IBVPs) for differential equations on graphs are used to describe many important processes in Physics and Engineering. As some examples, we mention mechanical vibrations of multi–linked flexible structures usually composed of flexible beams or strings, propagation of electro–magnetic waves in networks of optical fibers, heat flow in a wire mesh, and also electron flow in quantum mechanical circuits.

Graphs with differential equations on the edges (in particular, the Schrödinger equation) satisfying compatibility conditions at the inner vertices, have become known

‡ Research of this author was supported in part by the NSF, grant ARC 0724860.

§ Research of this author was supported in part by University of Tennessee at Chattanooga Faculty Research Grant.

‖ Research of this author was supported in part by University of Tennessee at Chattanooga Faculty Research Grant.

as quantum graphs. While the term "quantum graph" is relatively new (see, e.g. the survey [1]), the theory of partial differential equations on graphs has a rich history starting with pioneering papers by Lumer, von Below, Ali Mehmeti, and Nicaise, see, e.g. the books by Lagnese, Leugering and Schmidt [2], Dáger and Zuazua [3] and the survey [4]. Recent interest in quantum graphs is motivated, in particular, by possible applications to nano-electronics and quantum waveguides [5, 6].

Inverse problems (IPs) is an essential part of the quantum graph theory. Failure detection in mechanical multi-link structures by non-destructive methods as well as determination of their topological and material sensitivity with respect to a boundary observer is an important application of the inverse theory for partial differential equations on graphs. A solid theory of inverse problems for the Schrödinger equation on graphs would be an important step towards designing quantum devices (see, e.g. [7]).

Unfortunately, to date there are only a few results concerning IPs on graphs. The first question to be asked when studying the IP is how to establish the uniqueness result, i.e. to characterize spectral (or scattering or dynamical boundary) data ensuring a unique solution of the inverse problem. It was shown that inverse spectral and scattering problems for differential equations on graphs with cycles do not have in general a unique solution [8, 9, 10].

The first positive uniqueness results concerning IPs on graphs were obtained for trees (graphs without cycles). Brown and Weikard [11] and Yurko [12] proved uniqueness results for trees with a priori known topology (connectivity) and lengths of edges. Another group of results concerns inverse problems with unknown topology, lengths of edges and potentials. It includes the papers by Belishev and Vakulenko [13, 14], Avdonin and Kurasov [15] and Avdonin, Leugering and Mikhaylov [16].

A more detailed review of inverse uniqueness results on quantum tree can be found in [15].

The next important step after answering the uniqueness question is developing effective algorithms for solving IPs on graphs. At the moment there are no efficient algorithms for, or numerical experiments in, solving IPs on quantum graphs.

We now describe the *main challenges* one faces when approaching these problems.

Since the number of edges of graphs arising in applications is typically very big, one has to suggest a *recursive* procedure for solving the IP; this seems to be the only way for developing an effective numerical algorithm. For trees, this procedure should allow recalculating efficiently the inverse data from the original tree to the smaller trees, 'removing' leaves step by step up to the rooted edge.

Numerical tests for IPs are impossible without producing accurate inverse data. That means that one has to develop reliable numerical algorithms for solving the forward problems, i.e. *given the coefficients of the equations and the graph topology, find spectral and dynamical data of the quantum graph.*

Even for the simplest graphs, such as a finite interval or a semi–axis, solving of these (forward) problems is a rather difficult task from the numerical point of view. The surprising fact is that to solve numerically, say, the Gelfand–Levitan equation and

find the potential from the given spectral function (i.e., to solve the inverse problem) is much easier than to find the spectral function from the given potential (i.e., to solve the forward problem — to find the inverse data).

The same is true for inverse data of other kind (the Titchmarsh–Weyl function, scattering matrix or dynamical data).

The aforementioned difficulties increase dramatically for graphs with many edges.

Our approach to overcoming these difficulties is based on the Boundary Control (BC) method in inverse problems of mathematical physics. The characteristic feature of the BC method is its **locality**. Specifically, when applying the BC method to inverse problems on a finite interval or semi-axis, the recovery of a potential on a subinterval requires only the data related to that subinterval. Similarly, for inverse problems on graphs, the recovery of the topology and other parameters of a subgraph requires only the data related to that subgraph.

An efficient way for constructing inverse data was proposed in [17]. It reduced the problem of finding the response function by the given potential to a Volterra type integral equation. By the response function one can find the spectral function and the Titchmarsh–Weyl function as described in [18, 17].

A recursive procedure for the recovery of a tree's parameters was proposed in [15]. It allows recalculating efficiently, say, the Titchmarsh–Weyl function from the original tree to the smaller trees, "removing" leaves step by step up to the rooted edge.

This result was extended to the two-velocity wave equation (a model typical for elasticity theory) by Avdonin, Leugering and Mikhaylov [16]. In this model the lengths of the edges, speeds of the wave propagation, topology of the tree, and the angles between the edges had to be determined by boundary observations.

This recursive procedure can also be developed for dynamical inverse data; the first results in this direction were obtained in [15]. In this paper we construct algorithms and provide numerical experiments in solving IP on a simplest star-graph consisting of three edges using the dynamical data at one boundary vertex.

We pursue the following *goals*.

a) First we demonstrate efficiency of the BC method for solving IP on an interval and on the semi–axis. The celebrated Gelfand–Levitan and Krein equations have been well–known for solving this problem (see [18] for more detailed review). However, even for this simplest case we could not find developed algorithms in the literature. Some numerical results based on the BC method are presented in [19, 20, 21, 22]. However, at that time we did not know the efficient way to produce inverse data, i.e. solve the forward problem, and this is quite difficult (numerically). The paper [17] pawed the way to solving this problem.

b) We consider the wave equation on a star–graph with an unknown coordinate dependent potential on one edge and discuss IP of reconstruction of this potential. We derive a Volterra–type integral equation of the second kind that allows solving our IPs. Our approach involves the Dirichlet–to–Neumann map. We describe a numerical algorithm and conduct extensive numerical experiments. The graph consists of three

edges, two of which are semi-infinite. Control is applied to and an observation is made on the boundary of the finite edge and the potential is non-zero only on one of the semi-infinite edges. We recover it using the response operator observed on the boundary of the finite edge. For that, we recalculate the response function of the semi-infinite edge with a nontrivial potential (as if it were a separate string), using the response operator of the original system.

c) For both the Gelfand–Levitan problem and the problem on the star-graph, we present robust numerical implementations of the algorithms developed here. Each of these implementations consists of two distinct parts: a code for a forward problem (which generates a response function from a given potential) and a separate code for the corresponding inverse problem (which recovers a potential from a given response). The codes, developed with Matlab, have been extensively tested on example potentials including both smooth and discontinuous functions as well as potentials that simulate the addition of random noise in the system, as one might encounter in real-life data. On smooth data the code achieves second-order accuracy and the original potential can be recovered as precisely as required, and moreover the code appears capable of dealing with modest amounts of random noise. The forward problem is the most expensive, requiring computation time that grows like $O(n^4)$ on a grid of n points, but both the forward and inverse problems can be solved in a matter of minutes on a modern desktop computer.

The complete solution, including numerical implementation, of the IP for the aforementioned star–graph demonstrates the efficiency of our approach to inverse problems on graphs. We will address a general tree–graph situation in our sequel on this topic.

We now briefly describe the content of the paper. In Section 2, we give a brief overview of the BC method for solving IPs. In particular, we briefly describe the (known) connection between the potential and the response function that allows to find the kernel of the integral equation used for reconstruction. This fragment is needed to build a reliable method for the reconstruction algorithm. In Section 3, we formulate the IBVP on a graph and describe some auxiliary results. In Sections 4–6, we use the BC approach to solve our IPs, i.e. reconstruct the unknown potential. Specifically, in Section 4, we derive a representation of the solution to the IBVP in terms of the boundary control function. In Section 5, we derive two (dependent) Volterra integral equations of the second kind. One of them serves to prepare data for our numerical algorithm. Another equation represents one of the main objects of our study; it is needed for solving our IP. In Section 6, we analyze the solution of the auxiliary integral equation for small values of time. In Section 7, we give some auxiliary proofs. In Section 8, we describe a numerical algorithm of reconstruction and conduct extensive numerical experiments, including a study of the influence of noise on the reconstruction.

2. The Boundary Control approach to IP on the semi-axis.

The BC method uses the deep connection between IPs, functional analysis and control theory for partial differential equations and offers a powerful alternative to the previous identification techniques based on spectral or scattering methods. This approach has several advantages, namely: (i) it maintains linearity (does not introduce spurious nonlinearities); (ii) it is applicable to a wide range of linear systems and reconstruction situations; (iii) it allows one to identify coefficients occurring in highest order terms; (iv) it is, in principle, dimension–independent; and, finally, (v) it lends itself to straightforward algorithmic implementations. Being originally proposed for solving the boundary IP for the multidimensional wave equation, the BC method has been successfully applied to all main types of linear equations of mathematical physics (see the review papers [23, 24], monograph [25] and references therein). In this paper we use this method in a one-dimensional situation, applying it to the IP for the wave equation on the semi-axis and a simple star–graph. We consider here Dirichlet boundary conditions but note that this approach may be used for other boundary conditions as well (see, e.g. [26] for Neumann condition and [27] for a non–selfadjoint condition).

2.1. The initial boundary value problem and Goursat problem.

We consider the IBVP for the one-dimensional wave equation

$$\begin{cases} u_{tt}(x,t) - u_{xx}(x,t) + q(x)u(x,t) = 0, \quad x > 0,\ t > 0, \\ u(x,0) = u_t(x,0) = 0,\ u(0,t) = f(t). \end{cases} \tag{2.1}$$

Here $q \in L^1_{loc}(\mathbb{R}_+)$ and f is an arbitrary $L^2_{loc}(\mathbb{R}_+)$ function referred to as a *boundary control*. The solution $u^f(x,t)$ of the problem (2.1) can be written in terms of the integral kernel $w(x,s)$ which is the unique solution to the Goursat problem

$$\begin{cases} w_{tt}(x,t) - w_{xx}(x,t) + q(x)w(x,t) = 0, \quad 0 < x < t, \\ w(0,t) = 0,\ w(x,x) = -\frac{1}{2}\int_0^x q(s)\,ds. \end{cases} \tag{2.2}$$

The properties of the solution to the Goursat problem and its relation to the problem (2.1) are described by the following propositions.

Proposition 1 [18]

a) If $q \in L^1_{loc}(\mathbb{R}_+)$, then the generalized solution $w(x,s)$ to the Goursat problem (2.2) is a continuous function. Partial derivatives in (2.2) depend continuously in $L^1_{loc}(\mathbb{R}_+)$ on parameters x, s. The equation in (2.2) holds almost everywhere and the boundary conditions are satisfied in the classical sense.

b) If $q \in C_{loc}(\mathbb{R}_+)$, then the generalized solution $w(x,s)$ to the Goursat problem (2.2) is C^1-smooth, and both the equation and boundary conditions are satisfied in the classical sense.

c) If $q \in C^1_{loc}(\mathbb{R}_+)$, then the solution to the Goursat problem (2.2) is classical, and all its derivatives up to the second order are continuous.

Proposition 2 [28, 18]

a) If $q \in C^1(\mathbb{R}_+)$, $f \in C^2(\mathbb{R}_+)$ *and* $f(0) = f'(0) = 0$, *then*

$$u^f(x,t) = \begin{cases} f(t-x) + \int_x^t w(x,s) f(t-s)\, ds, & x \le t, \\ 0, & x > t. \end{cases} \tag{2.3}$$

is a classical solution to (2.1).

b) If $q \in L^1_{loc}(\mathbb{R}_+)$ *and* $f \in L^2_{loc}(\mathbb{R}_+)$, *supp* $f \subset [0,T]$, *then formula* (2.3) *represents a unique generalized solution* $u^f \in C([0,T]; \mathcal{H}^T)$ *to the IBVP (2.1) where*

$$\mathcal{H} = L^2_{loc}(0,\infty) \quad \text{and} \quad \mathcal{H}^T := \{u \in \mathcal{H} : \text{supp } u \subset [0,T]\}. \tag{2.4}$$

2.2. The main operators of the BC method.

The *response operator* (or the dynamical Dirichlet–to–Neumann map) R^T for the system (2.1) is defined on $\mathcal{F}^T := L^2(0,T)$ by

$$(R^T f)(t) = u^f_x(0,t), \quad t \in (0,T), \tag{2.5}$$

with the domain $\{f \in H^1(0,T) : \ f(0) = 0\}$. According to (2.3) it has a representation

$$(R^T f)(t) = -f'(t) + \int_0^t r(s) f(t-s)\, ds, \tag{2.6}$$

where $r(t) := w_x(0,t)$ is called the *response function*.

The response operator R^T is completely determined by the response function on the interval $[0,T]$, and the dynamical IP can be formulated as follows: *Given* $r(t)$, $t \in [0,2T]$, *find* $q(x)$, $x \in [0,T]$.

Notice that from (2.2) one can derive the formula (see [17] for details)

$$r(t) = -\frac{1}{2} q\Big(\frac{t}{2}\Big) - \frac{1}{2} \int_0^t q\Big(\frac{t-\zeta}{2}\Big) v(\zeta,t)\, d\zeta\,, \tag{2.7}$$

where

$$v(\xi,\eta) = w\Big(\frac{\eta-\xi}{2}, \frac{\eta+\xi}{2}\Big)\,.$$

Formula (2.7) implies that q and r have the same regularity.

The *connecting operator* $C^T : \mathcal{F}^T \mapsto \mathcal{F}^T$, plays the central role in the BC method. It connects the outer space (the space of controls) of a dynamical system (2.1) with the inner space (the space of solutions) being defined by its bilinear product:

$$\big\langle C^T f, g \big\rangle_{\mathcal{F}^T} = \big\langle u^f(\cdot,T), u^g(\cdot,T) \big\rangle_{\mathcal{H}^T}\,. \tag{2.8}$$

In other words,

$$C^T = (W^T)^* W^T\,, \tag{2.9}$$

and it is known [28, 18] that this operator is positive definite, bounded and boundedly invertible on $\mathcal{F}^T$.

The remarkable fact is that C^T can be explicitly expressed through R^{2T} (or through $r(t)$, $t \in [0,2T]$).

Proposition 3 [28, 18] *For $q \in L^1_{loc}(0,\infty)$ and $T > 0$, operator C^T has the form*

$$(C^T f)(t) = f(t) + \int_0^T c^T(t,s) f(s)\, ds\,,\ 0 < t < T\,, \tag{2.10}$$

where

$$c^T(t,s) = p(2T - t - s) - p(t - s) \tag{2.11}$$

and

$$p(t) = \frac{1}{2}\int_0^{|t|} r(s)\, ds. \tag{2.12}$$

2.3. The BC equations.

It has been proven [28] that one can recover the potential using the unique solution to any of the equations

$$(C^T f_0^T)(t) = T - t\,,\ \ (C^T f_1^T)(t) = -((R^T)^* \kappa^T)(t)\,,\ \ t \in [0,T]\,. \tag{2.13}$$

Here $(R^T)^*$ is the operator adjoint to R^T in $\mathcal{F}^T$:

$$((R^T)^* f)(t) = f'(t) + \int_t^T r(s-t) f(s)\, ds, \tag{2.14}$$

with the domain $\{f \in H^1(0,T) :\ f(T) = 0\}$ and $\kappa^T(t) := T - t$. Representation (2.10) allows rewriting equations (2.13) in the form:

$$f_0^T(t) + \int_0^T c^T(t,s)\, f_0^T(s)\, ds\ = T - t\,,\ t \in [0,T]\,, \tag{2.15}$$

$$f_1^T(t) + \int_0^T c^T(t,s)\, f_1^T(s)\, ds\ = 1 - \int_t^T r(s-t)\,(T-s)\, ds\,,\ t \in [0,T]\,. \tag{2.16}$$

From (2.15), (2.16) it follows that functions $f_j^T,\ j = 0, 1$, possess additional regularity, $f_j^T \in H^1(0,T)$.

Using any of functions f_j^T one can easily find the potential q as

$$q(T) = \frac{\mu_j''(T)}{\mu_j(T)}\,, \tag{2.17}$$

where $\mu_j(T) = f_j^T(+0)$.

Equations (2.13)–(2.17) were obtained for a matrix-valued q of a class C^1 in [28] and extended to q of a class L^1 in [18].

It is important to note that equation (2.15) is the Krein–type equation. More exactly, Krein in [29, 30] considered the problem with a Neumann boundary condition at $x = 0$. The equation similar to (2.15) corresponding to a Neumann boundary condition (see [26]) can be easily transformed to the Krein equation. A detailed discussion of relations between the Gelfand–Levitan [31], Krein, Simon [32], Remling [33, 34] and BC results can be found in [18].

2.4. Gelfand–Levitan theory

Determining the potential q from the spectral measure is the main result of the seminal paper by Gelfand and Levitan [31]. To formulate the result, we define the following functions:

$$\sigma(\lambda) = \begin{cases} \rho(\lambda) - \frac{2}{3\pi}\lambda^{\frac{3}{2}}, & \lambda \geqslant 0, \\ \rho(\lambda), & \lambda < 0, \end{cases} \tag{2.18}$$

$$F(x,t) = \int_{-\infty}^{\infty} \frac{\sin\sqrt{\lambda}x \sin\sqrt{\lambda}t}{\lambda}\, d\sigma(\lambda). \tag{2.19}$$

Let $\varphi(x,\lambda)$ be a solution to the equation

$$-\varphi'' + q(x)\varphi = \lambda\varphi, \quad x > 0, \tag{2.20}$$

with the Cauchy data

$$\varphi(0,\lambda) = 0, \quad \varphi'(0,\lambda) = 1. \tag{2.21}$$

The so–called transformation operator transforms the solutions of (2.20)–(2.21) with zero potential to the functions $\varphi(x,\lambda)$:

$$\varphi(x,\lambda) = \frac{\sin\sqrt{\lambda}x}{\sqrt{\lambda}} + \int_0^x K(x,t)\frac{\sin\sqrt{\lambda}t}{\sqrt{\lambda}}\, dt. \tag{2.22}$$

It was proved in [31] that the kernel $K(x,t)$ satisfies the integral (Gelfand–Levitan) equation

$$F(x,t) + K(x,t) + \int_0^x K(x,s)\, F(s,t)\, ds = 0\,, \quad 0 < t < x. \tag{2.23}$$

The potential can be recovered from the solution of this equation by the rule

$$q(x) = 2\frac{d}{dx}K(x,x). \tag{2.24}$$

In [18], using the BC approach, the local version of the classical Gelfand–Levitan equation (2.23) was derived:

$$V(x,t) + c^T(x,t) + \int_x^T c^T(t,s)V(x,s)\, ds = 0, \quad 0 < x < t < T. \tag{2.25}$$

Solving the equation (2.25) for all $x \in (0,T)$ we can recover the potential using

$$q(T-x) = -2\frac{dV(x,x)}{dx}. \tag{2.26}$$

It was shown in [18] that the kernel V is connected with the kernel of the transformation operator (2.22) by the rule $V(T-x,T-t) = K(x,t)$ and c^T is similarly related to F defined in (2.19): $c^T(T-x,T-t) = F(x,t)$. Therefore, equations (2.25) can be rewritten in a classical form (2.23). On the other hand, unlike (2.23) equation (2.25) has clearly a local character since $c^T(y,t)$ is completely determined by $q(y)$ on the interval $[0,T]$.

Remark. It appears that Equation (2.25) may be rewritten in another form, with the LHS having the same form as for $f_j^T(t)$ (see (2.15) and (2.16)). Indeed, the transformation

$$t-x=\tilde{t},\ s-x=\tilde{s},\ T-x=\tilde{T},\ \text{so that } 0<\tilde{t}<\tilde{T} \text{ and } V(x,x+\tilde{t})=F^{\tilde{T}}(\tilde{t}),$$

implies $c^T(x,t)=p(2T-x-t)-p(x-t)=p(2\tilde{T}-\tilde{t})-p(\tilde{t})$ and hence, for $0<\tilde{t}<\tilde{T}$,

$$F^{\tilde{T}}(\tilde{t})+\int_0^{\tilde{T}}(p(2\tilde{T}-\tilde{t}-\tilde{s})-p(\tilde{t}-\tilde{s}))F^{\tilde{T}}(\tilde{s})\,d\tilde{s}=p(\tilde{t})-p(2\tilde{T}-\tilde{t}).$$

We observe that indeed the LHS is of the same form as for f_j^T. Further, $V(x,x)=F^{\tilde{T}}(0+)$, $d/dx=-d/d\tilde{T}$ and hence,

$$q(\tilde{T})=-2\frac{dF^{\tilde{T}}(0+)}{d\tilde{T}}. \tag{2.27}$$

2.5. Finding the response function by the given potential.

Based on the results of [17] the problem of computing r by way of q reduces to a Volterra integral equation of the second kind.

Proposition 4 [17] *If $A(x,y)$ is the (unique) solution to the integral equation*

$$A(x,y)=q(x)-\int_0^y q(x-t)\Big(\int_t^x A(s,t)ds\Big)\,dt,\quad x,y>0, \tag{2.28}$$

then the function

$$\mathcal{A}(t)\equiv A(t,t) \tag{2.29}$$

satisfies

$$\mathcal{A}(t)=-2r(2t). \tag{2.30}$$

Hence, given the potential $q(x)$, we can find the response function $r(s)$ and the response operator R^T.

3. Statement of the IP for the wave equation on a specific tree. The main result on the response operator.

We consider the quantum graph (tree) $\mathbf{\Omega}$ that consists of three edges, $\mathbf{e}_1=\{x_1|0\le x_1\le l\}$, $\mathbf{e}_2=\{0\le x_2<\infty\}$, $\mathbf{e}_3=\{x_3|0\le x_3<\infty\}$ with one interior vertex $\gamma_0=\{x_1=x_2=x_3=0\}$ and one exterior vertex $\gamma_1=\{x_1=l\}$. See Figure 1. We study the IP for the wave equation on $\mathbf{\Omega}$,

$$u_{tt}-u_{xx}+q(x)u=0,\ (x,t)\in\mathbf{e}_j\times[0,\infty),\ j=1,2,3 \tag{3.1}$$

subject to the compatibility (so–called Kirchhoff) conditions at the vertex γ_0,

$$u_1(0,t)=u_2(0,t)=u_3(0,t),\ \sum_{j=1}^3 (u_j)_x(0,t)=0,\quad t\in[0,\infty), \tag{3.2}$$

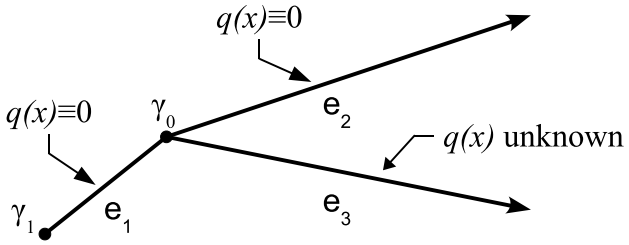

Figure 1. The quantum tree graph Ω.

zero initial conditions

$$u(x,0) = u_t(x,0) = 0,\ x \in \mathbf{\Omega}, \tag{3.3}$$

and the boundary condition at the vertex γ_1,

$$u_1(l,t) = f(t),\ t \in [0,\infty), \tag{3.4}$$

where the function $f(t)$ is said to be the *boundary control*.

We now introduce the response operator as in (2.5):

$$(R^T f)(t) = u^f_x(l,t), \quad t \in (0,T). \tag{3.5}$$

Physically, R^T may be viewed as a response to the signal $f(t)$ measured on an interval of time $(0,T)$.

Assumption. *The potential $q(x)$ is nontrivial on the edge $\mathbf{e}_3$ only, i.e. supp $q \subseteq \mathbf{e}_3$.*

Though this assumption definitely simplifies our consideration, it keeps the corresponding IBVP and IP nontrivial and yet allows us to present our reconstruction algorithm in a relatively simple form.

Our IP is formulated as follows. Given operator R^T to recover $q(x)$, $x \in [0,L]$. Since the speed of the wave propagation in the system (3.1)–(3.4) is equal to one, T, L and l are connected by the relation $T = 2(l+L)$. We propose an algorithm reconstructing the potential on the interval $[0,nl]$ with any positive integer n and the corresponding T equal to $2(n+1)l$. Numerical experiments are presented in Section 8 for $n = 2$.

The following result is well known for smooth potentials (see, e.g. [2], [35][Ch. VII]) and valid also for $q \in L^1$ [18].

Proposition 5. *Let $q \in L^1_{loc}(\mathbf{e}_3)$ and $f \in L^2(0,T)$. Then IBVP (3.1)–(3.4) has the unique solution $u \in C([0,T]; L^2(\mathbf{\Omega}))$.* •

The response operator of the system (3.1)–(3.4) does not have as simple a structure as the response operator for the wave equation on the semi-axis, as shown in (2.6). Therefore our first goal is to obtain a representation of the response operator R^T in terms of the response function of the wave equation on the edge $\mathbf{e}_3$ considered as a separate system.

To formulate the main result for the response operator, we have to introduce some objects. Let the function $p(t)$ be

$$p(t) = \frac{1}{2}\int_0^{|t|} r(s)ds, \quad \text{where } r(s) = w_x(0,s), \tag{3.6}$$

and the function $w(x,s)$ be the solution to the Goursat problem (see (2.2)) on the semi–infinite edge $\mathbf{e}_3$. Further let the operator K be defined as follows

$$(Kg)(t) = \frac{2}{3}\int_0^t p(t-s)g(s)ds \equiv \frac{2}{3}(p*g)(t). \tag{3.7}$$

We also introduce the shift type operator

$$(S\psi)(t) = \frac{2}{3}\sum_{k=1}^{\infty}\psi(t-2kl). \tag{3.8}$$

For any moment of time t, the number of terms in the sum above is finite.

We now formulate the main result for the response operator.

Theorem 1. *The response operator has the form*

$$(R^T f)(t) = (R^T f)^{(s)}(t) + (R^T f)^{(r)}(t), \tag{3.9}$$

where we let

$$(R^T f)^{(s)}(t) = \left(\left(I + 3S - 2S(I+S)^{-1}\left(I + \frac{3}{2}S\right)\right)f'\right)(t), \tag{3.10}$$

and

$$(R^T f)^{(r)}(t) = -\frac{1}{2}(S\Phi^{f'})(t). \tag{3.11}$$

The function $\Phi^{f'}$ is given by

$$\Phi^{f'}(t) \equiv 4\left(\left((I+S-K)^{-1} - (I+S)^{-1}\right)\left(I + \frac{3}{2}S\right)f'\right)(t). \tag{3.12}$$

We call $(R^T f)^{(s)}(t)$ the *singular part* of the response operator and $(R^T f)^{(r)}(t)$ the *regular part*. The regular part implicitly contains the function $r(t)$. It will be shown below that the knowledge of $(R^T f)^{(r)}$, actually the function $\Phi^{f'}(t)$ for $f(t) = \delta(t)$, is sufficient to reconstruct the unknown potential $q(x)$. The singular part is not of any help for our model. We note that for a general tree, with an unknown topology of the graph, the singular part allows reconstructing the number of vertices and the lengths of the edges. This fact may be observed from the structure of $(R^T f)^{(s)}(t)$ that contains the function f at the shifted moments of time $t - 2kl$ (with l to be the length of the edge $\mathbf{e}_1$.) For a general tree, the shifts that contain the lengths of all edges appear in the singular part of the response operator, thus making it quite informative.

The proof of Theorem 1 is multi–step and described in the next two sections. The main idea is to recalculate the inverse data (the measurement $(R^T f)(t)$ at the vertex γ_1) from the original graph $\mathbf{\Omega}$ to the edge $\mathbf{e}_3$ by "removing" two other edges, $\mathbf{e}_1$ and $\mathbf{e}_2$. After that, we can reconstruct the potential using the approach described in Section 2 for the IP on a semi–axis, in this case, the edge $\mathbf{e}_3$.

We further proceed as follows.

Step 1. Applying control $f(t)$ at the (lone) exterior vertex γ_1 and using the compatibility conditions (3.2) at the vertex γ_0, we find the general solution to the wave equation on all edges $\mathbf{e}_j$, $j = 1, 2, 3$. In particular, using compatibility conditions (3.2)

at the vertex γ_0 we find a representation for the solution on the edge $\mathbf{e}_3$ in terms of control $f(t)$.

Step 2. Derive a representation for the response operator.

Step 3. Using that representation we derive a Volterra integral equation of the second kind for the auxiliary function $p(t)$ (see (2.12) and (3.6) above) thus recalculating inverse data by effectively "removing" the edges $\mathbf{e}_2$, $\mathbf{e}_3$.

Step 4. Following the methodology of Section 2 we develop a numerical algorithm for solving the IP. See Section 8.

4. Step 1: General solution to the wave equation on the tree.

The proofs of the following two technical result are presented in Section 7.

Lemma 1. *The operators K and S defined by (3.7) and (3.8) have the following properties.*

a) For any continuous function φ and $s > 0$, $(K\varphi)(t-s) = (K\varphi(\xi-s))(t)$; $(K\varphi')(t-s) = K(\varphi'(\xi - s))(t)$. (Differentiability is required for the second identity.)

b) If $f(0) = 0$, then this representation holds:

$$(Kf')(t) = \frac{1}{6}\int_0^t r(t-s)f(s)ds. \tag{4.1}$$

c) The operators $I + S$ and $I - K + S$ are invertible.

d) The operators K and S commute on the integrable functions $\psi(t)$ such that $\psi(t) = 0$ for $t \le 0$.

We now describe the structure of the solution to the IBVP on the graph $\mathbf{\Omega}$.

Lemma 2. *1. The unique solution to the IBVP (3.1)–(3.4) has the form,*

$$u_1(x,t) = \sum_{k=0}^{\infty}\left(f(\tau + x - 2kl) - f(\tau - x - 2kl)\right) \tag{4.2}$$
$$+ g(\tau - x) - \sum_{k=1}^{\infty}\left(g(\tau + x - 2kl) - g(\tau - x - 2kl)\right)$$
$$u_2(x,t) = g(\tau - x), \tag{4.3}$$
$$u_3(x,t) = g(\tau - x) + \int_x^{\tau} w(x,s)g(\tau - s)ds. \tag{4.4}$$

Here τ is $t - l$ and the function g is uniquely defined by

$$g(\tau) = \frac{2}{3}\left((I - K + S)^{-1}\left(I + \frac{3}{2}S\right)f\right)(\tau). \tag{4.5}$$

5. Steps 2–3. Deriving a representation for the response operator and an integral equation for $p(t)$.

The response operator R^T is defined by (3.5). First, we prove the representation for it given by Theorem 1 (see (3.9), (3.10), (3.11), (3.12)).

Proof of Theorem 1. First, we use the representation (4.2) to find

$$(R^T f)(t) = f'(t) + 2\sum_{k=1}^{\infty} f'(t-2kl) - 2\sum_{k=1}^{\infty} g'(t-2kl). \tag{5.1}$$

Using the operator S given by (3.8) yields

$$(R^T f)(t) = f'(t) + 3(Sf')(t) - 3(Sg')(t). \tag{5.2}$$

We further use representation (4.5) to find

$$\begin{aligned}(R^T f)(t) = &\left(\left(I + 3S - 2S(I+S)^{-1}\left(I + \frac{3}{2}S\right)\right)f'\right)(t) \\ &-2\left(S\left((I-K+S)^{-1} - (I+S)^{-1}\right)\left(I+\frac{3}{2}S\right)\right)f'\Big)(t).\end{aligned} \tag{5.3}$$

Introducing the function $\Phi^{f'}$ by (3.12) yields the representation (3.9). Here we define the singular $(R^T f)^{(s)}(t)$ and regular $(R^T f)^{(r)}(t)$ parts of the response operator according to (3.10) and (3.11) correspondingly, and that completes the proof. •

Our next goal in this section is the derivation of an integral equation for the function $p(t)$ defined by (3.6) in terms of the solution to Goursat problem. As it was mentioned in Section 2, that equation will allow solving the IP, i.e. reconstructing $q(x)$. We will essentially use the arbitrariness of the function f.

We note first that the Equations (3.11) and (3.12) imply the following representation

$$(I-K+S)(R^T f)^{(r)}(t) = -\frac{4}{2}\left(S(I+\frac{3}{2}S)(I-I+K(I+S)^{-1})f'\right)(t). \tag{5.4}$$

We further apply the operator $I-K+S$ to the regular part $(R^T f)^{(r)}$ of the response operator given by (3.11) and use representation (5.4) to find

$$(I-K+S)(R^T f)^{(r)}(t)) = -\frac{1}{2}\left((I+S)S\Phi^{f'}\right)(t) + \frac{1}{2}\left(KS\Phi^{f'}\right)(t). \tag{5.5}$$

Combining representations (5.4) and (5.5) yields our *main equation*

$$\left((I+S)S\Phi^{f'}\right)(t) - (KS\Phi^{f'})(t) = 4\left(S\left(I+\frac{3}{2}S\right)K(I+S)^{-1}f'\right)(t). \tag{5.6}$$

On the interval of time $t \in [0, 2l)$ both sides of Equation (5.6) are identically equal to zero. We further consider the interval $t \in [2l, 4l)$, where Equation (5.6) has the form,

$$\Phi^{f'}(t-2l) - \frac{2}{3}\left(p * \Phi^{f'}(t-2l)\right)(t) = \frac{8}{3}\left(p * f'(t-2l)\right)(t) \tag{5.7}$$

or if we let $\eta \equiv t - 2l \in [0, 2l)$,

$$\Phi^{f'}(\eta) - \frac{2}{3}\left(p * \Phi^{f'}\right)(\eta) = \frac{8}{3}\left(p * f'\right)(\eta). \tag{5.8}$$

We further use the arbitrariness of the function f to choose

$$f'(\eta) = \delta(\eta). \tag{5.9}$$

Then Equation (5.8) admits the form,

$$p(\eta) + \frac{1}{4}\Big(\Phi^{\delta} * p\Big)(\eta) = \frac{3}{8}\Phi^{\delta}(\eta), \quad \eta \in [0, 2l). \tag{5.10}$$

It is further convenient to introduce the shift operator

$$(S_1\psi)(t) = \psi(t-2l), \tag{5.11}$$

so that

$$(S\psi)(t) = \frac{2}{3}\sum_{k=1}^{\infty}(S_1^k\psi)(t). \tag{5.12}$$

It is obvious that the combinations of the operator S that appear in Equation (5.6) may be explicitly written in terms of the shift operator,

$$\Big((I+S)S\psi\Big)(t) \equiv \sum_{k=1}^{\infty} a_k(S_1^k\psi)(t); \tag{5.13}$$

$$4\Big(S(I+\frac{3}{2}S)(I+S)^{-1})\psi\Big)(t) \equiv \sum_{k=1}^{\infty} b_k(S_1^k\psi)(t)$$

with some real coefficients $\{a_k\}$, $\{b_k\}$, $k \geq 1$. In particular

$$a_1 = \frac{2}{3},\ a_2 = \frac{10}{9},\ b_1 = \frac{16}{9},\ b_2 = \frac{64}{27}.$$

In fact, all coefficients may be found explicitly.

Hence if we consider the time interval $t \in [2nl, 2(n+1)l)$, then Equation (5.6) has the form

$$\sum_{k=1}^{n} a_k(S_1^k\Phi^{f'})(t) - \frac{4}{9}\sum_{k=1}^{n}(S_1^k(p*\Phi^{f'}))(t) = \sum_{k=1}^{n} b_k(S_1^k(p*f'))(t), \tag{5.14}$$

or with $\eta = t - 2l$,

$$\sum_{m=0}^{n-1} a_{m+1}(S_1^m\Phi^{f'})(\eta) - \frac{4}{9}\sum_{m=0}^{n-1}(S_1^m(p*\Phi^{f'}))(\eta) = \sum_{m=0}^{n-1} b_{m+1}(S_1^m(p*f'))(\eta). \tag{5.15}$$

With the choice (5.9), we find

$$\sum_{m=0}^{n-1}\frac{b_{m+1}}{b_1}(S_1^m p)(\eta) + \frac{4}{9b_1}\sum_{m=0}^{n-1}(S_1^m(\Phi^\delta * p))(\eta) = \sum_{m=0}^{n-1}\frac{a_{m+1}}{b_1}(S_1^m\Phi^\delta)(\eta). \tag{5.16}$$

In particular, if we further consider the next interval of time, $t \in [4l, 6l)$, then Equation (5.6) or (5.14) has the form,

$$\Big(\Phi^{f'}(\eta) + \frac{5}{3}\Phi^{f'}(\eta-2l)\Big) - \frac{2}{3}p*\Big(\Phi^{f'}(\eta) + \Phi^{f'}(\eta-2l)\Big) \tag{5.17}$$

$$= \frac{8}{3}(p*f')(\eta) + \frac{32}{9}f'(\eta-2l),\quad \eta\in[2l,4l)$$

or with the choice (5.9) and using (5.10),

$$p(\eta) + \frac{4}{3}p(\eta-2l) + \frac{1}{4}\Phi^\delta * \Big(p(\eta)+p(\eta-2l)\Big) \tag{5.18}$$

$$= \frac{3}{8}\Phi^\delta(\eta) + \frac{5}{8}\Phi^\delta(\eta-2l),\quad \eta\in[0,4l).$$

Equation (5.18) allows *two different interpretations.*

Interpretation 1. *If the function $p(t)$ is known, then Equation (5.18) may be viewed as a (Volterra type integral) equation for $\Phi^\delta(t)$,*

$$\Phi^\delta(\eta)+\frac{5}{3}\Phi^\delta(\eta-2l)-\frac{2}{3}\left(\left(p*\Phi^\delta\right)(\eta)+\left(p*\Phi^\delta\right)(\eta-2l)\right)=\frac{8}{3}p(\eta)+\frac{32}{9}p(\eta-2l) \quad (5.19)$$

Interpretation 2. *If the function $\Phi^\delta(t)$ is known, e.g. from measurements, then Equation (5.18) may be viewed as a (Volterra type integral) equation for $p(t)$. This will be the actual part of our numerical algorithm that determines the potential $q(x)$.*

Hence, given the potential $q(x)$, we may find the derivative of the Goursat function, $r(s) = w_x(0,s)$. That allows finding the function $\Phi^\delta(\eta)$, which represents our measurement, i.e. the regular part of the data $(R^T f)(t)$. In turn, knowing the data we may check our algorithm. The details on the *numerical algorithm* are described in Section 8.

6. Asymptotic behavior of $q(T)$ and $\mu(T)$ as $T \to 0$.

When considering a numerical implementation, the behavior of the solution near $T = 0$ is of importance. For this reason, we consider the equation analytically in this section.

We begin with Equation (2.15) and assume for simplicity that $r(t) \in C^1[0,T]$. Let $t = Tt'$, $t' \in (0,1)$, $f_0^T(t) \equiv f(t')$. Then

$$f(t')+T\int_0^1 (p(T(2-t'-s'))-p(T|t'-s'|))f(s')ds, = T(1-t'), \quad (6.1)$$

for $t' \in (0,1)$. As $T \to 0$, the last equation may be solved by iterations

$$f(t')=T(1-t)-T^2\int_0^1 (p(T(2-t'-s'))-p(T|t'-s'|))(1-s')ds' \quad (6.2)$$
$$+\cdots$$

In particular, for $f(0) = f_0^T(0+)$ we find

$$f(0)=T-T^2\int_0^1 (p(T(2-s'))-p(Ts'))(1-s')ds'+\cdots$$

Further

$$p(z)=\frac{1}{2}\int_0^z r(s)ds \asymp \frac{1}{2}r(0)z \text{ as } z\to 0$$

so that

$$p(T(2-s'))-p(Ts') \asymp \frac{1}{2}r(0)T(2-2s')$$

and hence

$$f(0)=T-\frac{T^3}{2}2r(0)\int_0^1 (1-s')^2ds'+o(T^3)=T-\frac{T^3}{3}r(0)+o(T^3). \quad (6.3)$$

But $r(s) = w_x(0,s)$, so $r(0) = w_x(0,0)$. Further

$$w(x,x)=-\frac{1}{2}\int_0^x q(s)ds$$

and

$$r(0) = -\frac{1}{2}\, q(0). \tag{6.4}$$

Finally

$$\mu(T) = f_0^T(0+) = f(0) = T + \frac{T^3}{6}\, q(0) + o(T^3) \tag{6.5}$$

and hence

$$\lim_{T\to 0} \frac{\mu''(T)}{\mu(T)} = \lim_{T\to 0} \frac{(T + \frac{T^3}{6}\, q(0))''}{T + \frac{T^3}{6}\, q(0)} = q(0) \tag{6.6}$$

which shows that computations in the neighborhood of $T = 0$ have to deal actually with an indeterminate form $0/0$.

We now consider Equation (2.7) for $t \to 0$. Substituting t for $2t$ and letting further $\xi = 2s$, $t - s = z$ yields instead of (2.7)

$$q(t) = 2r(2t) - 2\int_0^t q(z)v(2t - 2z, 2t)dz.$$

Using iterations in this Volterra type integral equation yields

$$\begin{aligned} q(t) = & -2r(2t) + 4\int_0^t v(2t - 2z, 2t)r(2z)dz + O(t^2) \\ = & -2r(0) - 4r'(0)t + O(t^2). \end{aligned} \tag{6.7}$$

7. Auxiliary proofs.

Proof of Lemma 1. The statements a) and b) may be checked by direct calculations. Indeed, if we consider the action of the operator K on $\varphi(\xi - s)$ (as always assume $\varphi(\xi - s) \equiv 0$ for $\xi \le s$), we find

$$\begin{aligned} (K\varphi(\xi - s))(t) &= \frac{1}{3}\int_s^t p(t - \xi)\varphi(\xi - s)d\xi \\ &= \frac{1}{3}\int_0^{t-s} p(t - s - \tau)\varphi(\tau)d\tau \\ &= (K\varphi(\xi))(t - s), \end{aligned} \tag{7.1}$$

so that the statement a) holds. For b), we have

$$\begin{aligned} (Kf')(t) &= \frac{1}{3}\int_0^t p(t - s)f'(s)ds \\ &= \frac{1}{3}\, p(t - s)f(s)|_0^t + \frac{1}{3}\int_0^t p'(t - s)f(s)ds \end{aligned} \tag{7.2}$$

The substitution at $s = t$ vanishes due to $p(0) = 0$ and at $s = 0$ due to $f(0) = 0$:

$$(Kf')(t) = \frac{1}{6}\int_0^t r(t - s)f(s)ds.$$

c) Invertibility of the operator $I-K+S$ appears as follows. First, we formally find

$$(I-K+S)^{-1}=((I+S)(I-(I+S)^{-1}K))^{-1}=(I-(I+S)^{-1}K)^{-1}(I+S)^{-1}.$$

The operator K is the Volterra integral operator, which implies invertibility of $I-(I+S)^{-1}K$ (see [36], Ch. IV, Section 32). Invertibility of $I+S$ may be checked directly from the formula

$$(I+S)^{-1}=I-S+S^2-...$$

where the number of terms is finite for any moment of time t.

d) We find

$$\begin{aligned}(KS\psi)(t)&=\frac{2}{3}\int_0^t p(t-s)(S\psi)(s)ds\\&=\frac{4}{9}\int_0^t p(t-s)\sum_{k=1}^{\infty}\psi(s-2kl)ds\\&=\frac{4}{9}\sum_{k=1}^{\infty}\int_{-2kl}^{t-2kl}p(t-2kl-s)\psi(s)ds\\&=\frac{4}{9}\sum_{k=1}^{\infty}\int_{0}^{t-2kl}p(t-2kl-s)\psi(s)ds\\&=\frac{2}{3}\sum_{k=1}^{\infty}\left(\frac{2}{3}\int_0^t p(t-s)\psi(s)ds)\right)\Bigg|_{t\to t-2kl}=(SK\psi)(t).\ \bullet\end{aligned}$$

Proof of Lemma 2. 1. The solution to the wave equation (3.1) on the graph $\mathbf{\Omega}$ subject to the boundary condition (3.4) may be given in terms of the solution $w(x,t)$ to the Goursat problem and two arbitrary (smooth) functions g, g_1 (see e.g. [37], Lecture IV, Section 3 or [38]),

$$\begin{aligned}u_1(x,t)&=f(\tau+x)+g_1(\tau-x)\\&\quad-\sum_{k=1}^{\infty}\left(g_1(\tau+x-2kl)-g_1(\tau-x-2kl)\right),\end{aligned}\tag{7.3}$$

$$u_2(x,t)=g(\tau-x),\tag{7.4}$$

$$u_3(x,t)=g(\tau-x)+\int_x^{\tau}w(x,s)g(\tau-s)ds,\tag{7.5}$$

where $\tau\equiv t-l$. It is assumed that $g(s)=g_1(s)=0$ for $s\le 0$. The number of terms in (7.3) increases with time t, yet is finite for any given moment of time.

The representation (7.3) satisfies the boundary condition (3.4). Indeed,

$$\begin{aligned}u_1(l,t)&=f(t)+g_1(t-2l)-g_1(t-2l)+g_1(t-4l)+g_1(t-6l)\\&\quad-g_1(t-4l)-g_1(t-6l)+g_1(t-8l)-\cdots\\&=f(t).\end{aligned}$$

Compatibility (Kirchhoff) conditions (3.2) imply two connections between g and g_1. To derive the corresponding equations, we note first that the sums in (7.3) have the

properties

$$\sum_{k=1}^{\infty} (g_1(\tau + x - 2kl) - g_1(\tau - x - 2kl))\Big|_{x=0} = 0;$$

$$\frac{d}{dx} \sum_{k=1}^{\infty} (g_1(\tau + x - 2kl) - g_1(\tau - x - 2kl))\Big|_{x=0} = 2\sum_{k=1}^{\infty} g_1'(\tau - 2kl).$$

Hence,

$$f(\tau) + g_1(\tau) = g(\tau), \tag{7.6}$$

and

$$f'(\tau) - g_1'(\tau) - 3(Sg_1')(\tau) - 2g'(\tau) \tag{7.7}$$
$$-w(x,x)g(\tau - x)|_{x=0} + \int_0^\tau w_x(0,s)g(\tau - s)ds = 0,$$

where the substitution vanishes since $w(0,0) = 0$.

Equations (7.6), (7.7) allow representing the functions g and g_1 in terms of the control $f(t)$ only, thus effectively "removing" the edges $\mathbf{e}_2$, $\mathbf{e}_3$.

To this end, we integrate Equation (7.7), use the definition (3.6) and the calculation

$$\int_0^\tau \int_0^z w_x(0,s)g(z-s)dsdz = \int_0^\tau g(\xi) \int_0^{\tau-\xi} r(s)dsd\xi$$
$$= 2\int_0^\tau g(\xi)p(\tau - \xi)d\xi = 2(p * g)(\tau)$$

to find

$$f(\tau) - g_1(\tau) + 2(p * g)(\tau) - 3(Sg_1)(\tau) - 2g(\tau) = 0. \tag{7.8}$$

Substituting $g_1(\tau) = g(\tau) - f(\tau)$ from Equation (7.6) into Equation (7.8) yields

$$(I - K + S)g(\tau) = \frac{2}{3}\left(I + \frac{3}{2}S\right) f(\tau). \tag{7.9}$$

This equation is uniquely solvable for $g(\tau)$,

$$g(\tau) = \frac{2}{3}\left((I + S - K)^{-1}\right)\left(I + \frac{3}{2}S\right) f(\tau) \tag{7.10}$$
$$= \frac{2}{3}(I + S)^{-1}\left(I + \frac{3}{2}S\right) f(\tau) + K_1 f(\tau)$$

where we introduce the operator

$$K_1 \equiv \frac{2}{3}\left((I + S - K)^{-1} - (I + S)^{-1}\right)\left(I + \frac{3}{2}S\right). \tag{7.11}$$

The operator K_1 is compact as a convergent series of compact operators (see [36], Ch. IV, Section 32).

We now express the function g_1 in terms of f based on (7.6) and combine the formulas for g and g_1 with the representation (7.3)–(7.5), and that completes the proof. •

8. Numerical experiments.

In the above we have outlined algorithms for two the forward and inverse problems. The approaches described provide not just theoretical means for recovering an unknown potential q, but in fact practical algorithms which can be implemented numerically. Below we present the results of working Matlab codes which demonstrate this result.

8.1. Numerical aspects of the Gelfand–Levitan theory

In this section we provide the details of the numerical algorithm for solving the IP (in particular, finding $q(x)$) on a semi–axis. The algorithm is based on the local version of the Gelfand–Levitan approach [18].

Our numerical treatment has two parts. First a code simulates the forward problem and generates a response function $r(t)$ given the potential q. The function $p(t)$ is found by direct integration. A distinct second code for the inverse problem takes as input only the function p and its domain, and from that data reconstructs the potential q on its respective domain.

The forward problem is solved in the following way.

(i) A potential q is given over a particular domain, say $x \in (0, 2l)$ where $l = 1$ or π. We consider potentials like $q(x) = 4x$ and $q(x) = \sin(4x)$.

(ii) The integral equation (2.28) is solved for $A(\alpha, \beta)$. That is, we numerically determine A from

$$A(x, y) = q(x) - \int_0^y q(x - t) \left(\int_t^x A(s, t)\, ds \right) dt$$

for $x, y \in (0, 2l)$. The double integral is discretized with a two-dimensional composite interpolatory quadrature, specifically the two-dimensional trapezoidal rule, a second order method. (For this and the other quadratures used here, see for example [39].)

(iii) The A-amplitude $\mathcal{A}(t)$ is computed through the relation

$$\mathcal{A}(t) \equiv A(t, t)$$

for $t \in (0, 2l)$.

(iv) The function r is determined on its domain $(0, 4l)$ through the relation

$$r(s) = -\frac{1}{2}\mathcal{A}\left(\frac{s}{2}\right).$$

(v) The function p is an antiderivative of r for which $p(0) = 0$ and the composite trapezoidal rule is used to evaluate

$$p(\tau) = \frac{1}{2}\int_0^\tau r(s)\, ds$$

on the domain $\tau \in (0, 4l)$.

If given the function p defined on $(0, 4l)$ the potential can be numerically computed on $(0, 2l)$ through the following implementation of the inverse problem.

(i) Given p defined on a mesh of points in $(0, 4l)$ we compute V by numerically solving

$$V(y,t) + \int_y^T \left(p\left(2T - t - s\right) - p\left(|t - s|\right)\right) V(y,s)ds = p\left(|y - t|\right) - p\left(2T - y - t\right)$$

for $T \in (0, 2l)$ and $0 \leq y \leq t \leq T$. For a given value of T and a value of y the equation above is discretized using a trapezoidal rule and a linear system is formed for the values of the unknown function $V(y, \cdot)$ on the domain $[y, T]$. As above, the method given here is second order.

(ii) Finally the potential q is recovered through the formula

$$q(x) = 2\frac{d}{dx}V(T - x, T - x)$$

using a second order finite difference formula.

We offer the following comments to understand the above algorithm, its implementation, and the results given below.

- Note that q is recovered on half the interval of p, just as in the forward problem p is defined over twice the interval of the original q.
- The solution of each integral equation above, in one dimension or two, is achieved through some implementation of the trapezoidal rule.
- Nominally these methods are second order accurate. The estimated order for the method is recorded in the tables below, as a standard check of empirical results against the theoretical expectations. That is, we estimate the rate of convergence as the logarithm base 2 of the ratio of two successive error estimates when the number of discretization points is doubled.

Results for various potentials are given below. The 2-norm given here is a numerical approximation of the L^2 norm of the functions using a trapezoidal rule for the quadrature. The ∞-norm given here is the maximum of the modulus, taken pointwise, naturally.

In each example below the domains are the same for both the original potential q, used to generate the response function r, and the recovered potential, $\hat{q}$. In particular, we take $l = 1$ and q and $\hat{q}$ defined on $(0, 2)$ for all of the computations. Moreover n will refer to the number of points in the discretization of the domain.

The simplest potential we consider is a linear function, and the results are empirically second-order, as expected.

We also considered various oscillatory potentials, such as the following $q(x) = \sin(4x)$. The potential completes more than one period in the domain of the potential, and we are able to recover the entire function with our algorithm and corresponding code with complete second order accuracy. The original potential and the recovered potential are shown in Figure 2.

We further considered a step function as an example of a discontinuous potential. The results show that we get pointwise convergence away from the discontinuity, but that at the discontinuity there is a difference which stays large despite refinement of the discretization.

Table 1. Numerical convergence results for the potential $q(x) = 4x$.

n	$\|q - \hat{q}\|_2$	Est. Order	$\|q - \hat{q}\|_\infty$	Est. Order
50	6.9427×10^{-2}	—	2.1249×10^{-1}	—
100	1.8198×10^{-2}	1.932	5.6168×10^{-2}	1.920
200	4.6597×10^{-3}	1.965	1.4420×10^{-2}	1.962
400	1.1791×10^{-3}	1.983	3.6520×10^{-3}	1.981
800	2.9655×10^{-4}	1.991	9.1885×10^{-4}	1.991

Table 2. Numerical convergence results for the potential $q(x) = \sin(4x)$.

n	$\|q - \hat{q}\|_2$	Est. Order	$\|q - \hat{q}\|_\infty$	Est. Order
50	1.5373×10^{-3}	—	1.5734×10^{-3}	—
100	3.8656×10^{-4}	1.992	3.9531×10^{-4}	1.997
200	9.6885×10^{-5}	1.996	9.8847×10^{-5}	2.000
400	2.4250×10^{-5}	1.998	2.4715×10^{-5}	2.000
800	6.0662×10^{-6}	1.999	6.1788×10^{-6}	2.000

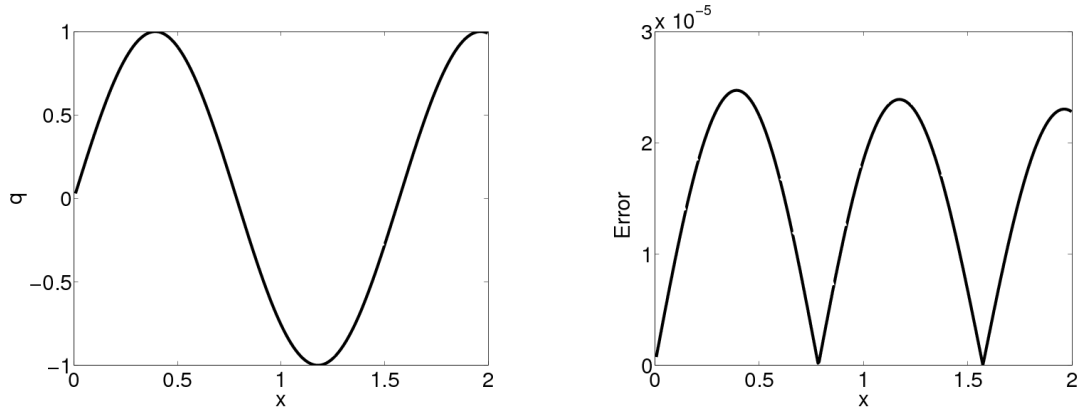

Figure 2. Numerical recovery of a sinusoidal potential, $q(x) = \sin(4x)$. Left: Recovered potential, nearly identical to original potential. Right: Absolute error between original and recovered potentials.

Table 3. Numerical convergence results for a step-potential. $q(x) = 2$ for $x < 1$ and $q(x) = 1$ for $x > 1$

n	$\|q - \hat{q}\|_2$	Est. Order	$\|q - \hat{q}\|_\infty$	Est. Order
50	5.0093×10^{-2}	—	2.5045×10^{-1}	—
100	3.5372×10^{-2}	0.502	2.5012×10^{-1}	—
200	2.5003×10^{-2}	0.501	2.5003×10^{-1}	—
400	1.7678×10^{-2}	0.500	2.5001×10^{-1}	—
800	1.2500×10^{-2}	0.500	2.5000×10^{-1}	—

8.2. Numerical aspects for the Inverse Problem on a Star Graph

Our numerical method for the inverse problem on a star graph is related to the one described above for the Gelfand–Levitan theory. As before, we consider a potential q

and through the forward problem obtain the auxiliary function Φ. Subsequently we solve the inverse problem using only Φ as data, and thereby recover the potential q. In closing, we also consider the influence of noise on the algorithm.

The forward problem is solved in the following way. The key addition here is the computation of the auxiliary function Φ.

(i) A potential q is given over a particular domain, say $x \in (0, 2l)$ where $l = 1$ or π. We consider potentials like $q(x) = 4x$ and $q(x) = \sin(4x)$.

(ii) The integral equation (2.28) is solved for $A(x, y)$. That is, we numerically determine A from

$$A(x,y) = q(x) - \int_0^y q(x-t)\left(\int_t^x A(s,t)\,ds\right)dt$$

for $x, y \in (0, 2l)$. The double integral is discretized with a two-dimensional composite interpolatory quadrature, specifically the two-dimensional trapezoidal rule, a second order method. (For this and the other quadratures used here, see for example [39].)

(iii) The A-amplitude $\mathcal{A}(t)$ is computed through the relation

$$\mathcal{A}(t) \equiv A(t,t)$$

for $t \in (0, 2l)$.

(iv) The function r is determined on its domain $(0, 4l)$ through the relation

$$r(s) = -\frac{1}{2}\mathcal{A}\left(\frac{s}{2}\right).$$

(v) The function p is an antiderivative of r for which $p(0) = 0$ and the composite trapezoidal rule is used to evaluate

$$p(\tau) = \frac{1}{2}\int_0^\tau r(s)\,ds$$

on the domain $\tau \in (0, 4l)$.

(vi) Finally, the function Φ is recovered by solving the Volterra equation of the second kind

$$\Phi(\eta) + \frac{5}{3}\Phi(\eta - 2l) - \frac{2}{3}\left((p * \Phi)(\eta) + (p * \Phi)(\eta - 2l)\right) = \frac{8}{3}p(\eta) + \frac{32}{9}p(\eta - 2l)$$

on the domain $\eta \in (0, 4l)$, see (5.19). In particular a trapezoidal rule can be applied to this equation in order to determine the solution numerically. The smooth problems considered here are covered by the theory given in [40] and therefore this method is known to be second order accurate.

Given the function Φ defined on $(0, 4l)$ the potential can be numerically computed on $(0, 2l)$ through the following implementation of the inverse problem.

(i) Given Φ defined on a mesh of points in $(0, 4l)$ we compute p by numerically solving

$$p(\eta) + \frac{4}{3}p(\eta - 2l) + \frac{1}{4}\Phi^\delta * \Big(p(\eta) + p(\eta - 2l)\Big) = \frac{3}{8}\Phi^\delta(\eta) + \frac{5}{8}\Phi^\delta(\eta - 2l)$$

for $\eta \in (0, 4l)$, see (5.18). This is another Volterra equation of the second kind, and as with the computation of Φ in the forward problem, the solution is found via a second order accurate trapezoidal method.

(ii) We solve the integral equation (2.15) for the function f^T defined for $t \in (0, 2l)$. That is

$$f^T(t) + \int_0^T \left(p(2T - t - s) - p\left(|t - s|\right)\right) f^T(s)\, ds = T - t$$

for all $T \in (0, 2l)$ and $0 \leq t \leq T$. For each T the equation above is discretized using a trapezoidal rule and a linear system is formed for the values of the unknown function f^T on the domain $[0, T]$. Only the value of $f^T(0)$ for each value of T is required for subsequent calculations.

(iii) The function μ is defined through the relation

$$\mu(T) \equiv f^T(0)$$

and then the potential q is recovered through the formula

$$q(T) = \frac{\mu''(T)}{\mu(T)}$$

using finite differences. The methods used above are nominally second order in interior of the domain, but the current treatment at the boundary makes the method only first order near the endpoints. A more delicate treatment of these end cases should result in a method which is fully second order.

We offer the following comments to understand the above algorithm, its implementation, and the results given below.

- Note that q is recovered on half the interval of Φ, just as in the forward problem Φ is defined over twice the interval of the original q.
- The solution of each integral equation above, in one dimension or two, is achieved through some implementation of the trapezoidal rule. Nominally these methods are second order accurate.
- Nominally these methods are second order accurate. The tables show the estimated order, as was done for the numerical computations for the Gelfand–Levitan approach in the previous section.
- Internally most pieces of the method achieve second order accuracy. For example, the computation of p from r is second order accurate in practice. More importantly, if we take a given p and compute Φ in the forward problem and then use the first part of the inverse problem to recover p, the results are second order accurate.

In each example below the domains are the same for both the original potential q, used to generate the function Φ, and the recovered potential, $\hat{q}$. In particular, we take $l = 1$ and therefore q and $\hat{q}$ defined on $(0, 2)$ for all of the computations. Moreover n will refer to the number of points in the discretization of the domain.

Table 4. Numerical convergence results for the potential $q(x) = 4x$.

n	$\|q - \hat{q}\|_2$	Est. Order	$\|q - \hat{q}\|_\infty$	Est. Order
50	5.5256×10^{-2}	—	1.7245×10^{-1}	—
100	1.5232×10^{-2}	1.859	4.7819×10^{-2}	1.851
200	4.0285×10^{-3}	1.919	1.2596×10^{-2}	1.925
400	1.0475×10^{-3}	1.943	3.2326×10^{-3}	1.962
800	2.7826×10^{-4}	1.912	1.3588×10^{-3}	1.250

Table 5. Numerical convergence results for the potential $q(x) = \sin(4x)$.

n	$\|q - \hat{q}\|_2$	Est. Order	$\|q - \hat{q}\|_\infty$	Est. Order
50	4.9311×10^{-3}	—	1.7936×10^{-2}	—
100	1.8486×10^{-3}	1.415	9.7387×10^{-3}	0.881
200	6.8389×10^{-4}	1.434	4.9672×10^{-3}	0.971
400	2.4808×10^{-4}	1.463	2.4959×10^{-3}	0.993
800	8.8949×10^{-5}	1.480	1.2495×10^{-3}	0.998

The simplest potential we consider is a linear function, and the results are empirically second-order, as expected. The only exception is the case $n = 800$ where the effect of a first-order treatment at one boundary begins to affect the error in the ∞-norm. The recovered potential and the absolute error for the case $n = 400$ are shown in Figure 3.

We also considered various oscillatory potentials, such as the following $q(x) = \sin(4x)$. The potential completes more than one period in the domain of the potential, and we are able to recover the entire function with our algorithm and corresponding code with better than first order accuracy in the 2-norm. The first-order accuracy of the boundary treatment is clearly visible in the ∞-norm results.

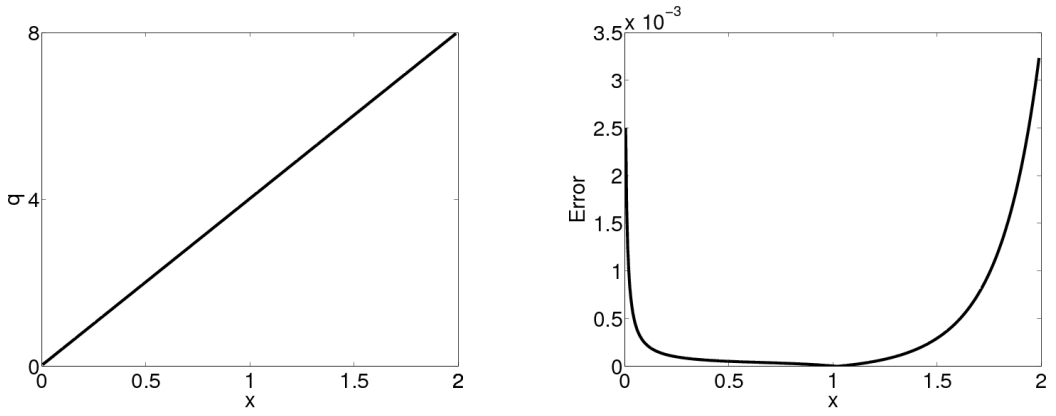

Figure 3. Numerical recovery of linear potential, $q(x) = 4x$. Left: Recovered potential, nearly identical to original potential. Right: Absolute error between original and recovered potentials.

Table 6. Numerical convergence results for a step potential. $q(x) = 2$ for $x < 1$ and $q(x) = 1$ for $x > 1$

n	$\|q - \hat{q}\|_2$	Est. Order	$\|q - \hat{q}\|_\infty$	Est. Order
50	6.2200×10^{-2}	—	3.0393×10^{-1}	—
100	4.4532×10^{-2}	0.482	3.0831×10^{-1}	—
200	3.1680×10^{-2}	0.491	3.1043×10^{-1}	—
400	2.2468×10^{-2}	0.496	3.1147×10^{-1}	—
800	1.5911×10^{-2}	0.498	3.1199×10^{-1}	—

We further considered a step function as an example of a discontinuous potential. The results show that we get pointwise convergence away from the discontinuity, but that at the discontinuity there is a difference which stays large despite refinement of the discretization.

It is important to note the efficiency of the algorithm which reconstructs the potential q from the function p. The first half of the algorithm described above, which constructs the function p (and then the auxiliary function Φ) from a given potential q, is extremely expensive in its current implementation, with computation time growing at a rate approaching $O(n^4)$. On a modest GNU/Linux machine with a 2.3GHz processor, the direct simulation of Φ for the case $n = 200$ takes well over four minutes to complete.

While the execution time does grow like $O(n^3)$ for the inverse problem, i.e. the computation of q from a given function p (obtained from Φ), the run times are significantly less. For example, the reconstruction of q from p when $n = 200$ takes only 9 seconds on the same 2.3GHz GNU/Linux machine.

We have also considered the case in which noise appears in the function Φ, as might occur in an actual experiment, in order to determine whether the algorithm set out here tolerates such perturbations. In particular, we constructed from Φ a noisy function $\hat{\Phi}(t) = \Phi(t) + \epsilon n(t)$ where $-1 \leq n(t) \leq 1$ has uniformly distributed random values and $\epsilon > 0$ is a small positive value.

As a specific example of the results we obtain, we used the sinusoidal potential $q(x) = \sin(4x)$, numerically simulated the function Φ, and constructed $\hat{\Phi}$ as above with $\epsilon = 0, 2.5 \times 10^{-3}$, and 1×10^{-2}. In Figure 4 the results are presented. As the magnitude of the perturbation of Φ is increased, the reconstructed $\hat{q}$ is correspondingly perturbed, although there is a nontrivial constant magnification of the perturbation. In the specific example of Figure 4 the perturbation of q (as measured in the L^2-norm) is approximately 48ϵ for all cases shown.

References

[1] P Kuchment. Quantum graphs: an introduction and a brief survey. In P Exner, J Keating, P Kuchment, T Sunada, and A Teplyaev, editors, *Analysis on Graphs and its Applications*, volume 77 of *Proceedings of Symposia in Pure Mathematics*, Providence, RI, 2008. Amer. Math. Soc.

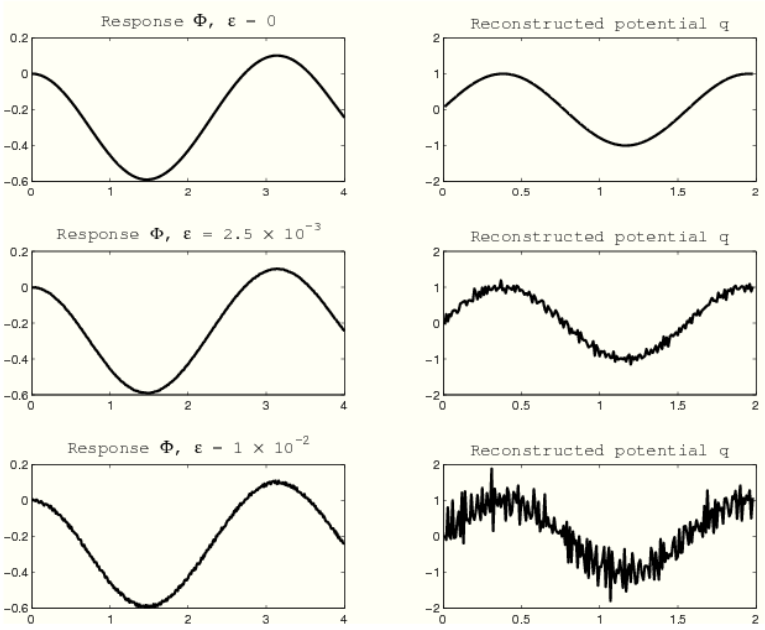

Figure 4. The effect that noise in Φ has on the reconstructed potential $\hat{q}$.

[2] J E Lagnese, G Leugering, and E J P G Schmidt. *Modelling, Analysis and Control of Multi-Link Flexible Structures*. Birkhauser, Basel, 1994.

[3] R Dager and E Zuazua. Wave propagation, observation and control in 1-*d* flexible multi-structures. *Mathematiques and Applications*, 50, 2006.

[4] S Avdonin. Control problems on quantum graphs. In *Analysis on Graphs and Its Applications*, volume 77 of *Proceedings of Symposia in Pure Mathematics*, pages 507–521. AMS, 2008.

[5] S Albeverio and P Kurasov. *Singular Perturbations of Differential Operators. Solvable Schroedinger Type Operators*, volume 271 of *London Mathematical Society Lecture Note Series*. Cambridge University Press, Cambridge, 2000.

[6] P Kuchment. Quantum graphs. I. Some basic structures. Special section on quantum graphs. *Waves Random Media*, 14(1):291–312, 2004.

[7] V Kostrikin and R Schrader. Kirchoff's rule for quantum wires II: the inverse problem with possible applications to quantum computers. *Fortschritte der Physik*, 48:703–716, 2000.

[8] T Kottos and U Smilansky. Periodic orbit theory and spectral statistics for quantum graphs. *Ann. Physics*, 274(1):76–124, 1999.

[9] B Gutkin and U Smilansky. Can one hear the shape of a graph? *J. Phys. A.*, 34(31):6061–6068, 2001.

[10] P Kurasov and M Nowaczyk. Inverse spectral problem for quantum graphs. *J. Phys. A*, 38(22):4901–4915, 2005.

[11] B M Brown and R Weikard. A borg–levinson theorem for trees. In *Proc. R. Soc. Lond. Ser. A Math. Phys. Eng. Sci.*, volume 461, pages 3231–3243, 2005.

[12] V. Yurko. Inverse Sturm-Liouville operator on graphs. *Inverse Problems*, 21:1075–1086, 2005.

[13] M Belishev. Boundary spectral inverse problem on a class of graphs (trees) by the BC method. *Inverse Problems*, 20:647–672, 2004.

[14] M I Belishev and A F Vakulenko. Inverse problems on graphs: recovering the tree of strings by the BC-method. *J. Inv. Ill-Posed Problems*, 14:29–46, 2006.

[15] S A Avdonin and P Kurasov. Inverse problems for quantum trees. *Inverse problems and imaging*, 2(1):1–21, 2008.
[16] S A Avdonin, G Leugering, and V Mikhaylov. On an inverse problem for tree-like networks of elastic strings. *Zeit. Angew. Math. Mech.*, 90:136–150, 2010.
[17] S A Avdonin, V Mikhaylov, and A Rybkin. The boundary control approach to the Titchmarsh-Weyl $m-$function. *Comm. Math. Phys.*, 275(3):791–803, 2007.
[18] S A Avdonin and V Mikhaylov. Boundary control approach to inverse spectral theory. *Inverse Problems*, 26:1–19, 2010.
[19] M I Belishev and A P Kachalov. The methods of boundary control theory in the inverse spectral problem for an inhomogeneous string. *J. Soviet Math.*, 57(3):3072–3077, 1991.
[20] M I Belishev and T L Sheronova. Methods of boundary control theory in a nonstationary inverse problem for an inhomogeneous string. *J. Math. Sci.*, 73:320–329, 1995.
[21] S A Avdonin, M I Belishev, and Yu S Rozhkov. The BC–method in the inverse problem for the heat equation. *J. Inverse and Ill-Posed Problems*, 5:309–322, 1997.
[22] S A Avdonin, M I Belishev, and Yu S Rozhkov. A dynamic inverse problem for the nonselfadjoint Sturm–Liouville operator. *J. Math. Sci.*, 102(4):4139–4148, 2000.
[23] M I Belishev. Boundary control in reconstruction of manifolds and metrics (the BC method). *Inverse Problems*, 13(5):R1–R45, 1997.
[24] M I Belishev. Recent progress in the boundary control method. *Inverse Problems*, 23(5):R1–R67, 2007.
[25] A Katchalov, Ya Kurylev, and M Lassas. *Inverse Boundary Spectral Problems*. Chapman Hall/CRC, Boca Raton, FL, 2001.
[26] S A Avdonin, S Lenhart, and V Protopopescu. Solving the dynamical inverse problem for the Schroedinger equation by the boundary control method. *Inverse Problems*, 18:349–361, 2002.
[27] S Avdonin and L Pandolfi. Boundary control method and coefficient identification in the presence of boundary dissipation. *Applied Math. Letters*, 22(11):1705–1709, 2009.
[28] S A Avdonin, M I Belishev, and S A Ivanov. Boundary control and inverse matrix problem for the equation $u_{tt} - u_{xx} + V(x)u = 0$. *Math. USSR Sbornik*, 7:287–310, 1992.
[29] M G Krein. A transmission function of a second order one-dimensional boundary value problem. *Dokl. Akad. Nauk. SSSR*, 88(3):405–408, 1953.
[30] M G Krein. On the one method of effective solving the inverse boundary value problem. *Dokl. Akad. Nauk. SSSR*, 94(6):987–990, 1954.
[31] I M Gel'fand and B M Levitan. On the determination of a differential equation from its spectral function. *Izvestiya Akad. Nauk SSSR. Ser. Mat.*, 15:309–360, 1951. in Russian, Amer. Math Soc. Transl. (2) 1 253–304.
[32] B Simon. A new approach to inverse spectral theory, I. Fundamental formalism. *Annals of Mathematics*, 150:1029–1057, 1999.
[33] C Remling. Inverse spectral theory for one–dimensional Schroedinger operators: the A function. *Math. Z.*, 245:597–617, 2003.
[34] C Remling. Schroedinger operators and de Branges spaces. *J. Funct. Anal.*, 196(2):323–394, 2002.
[35] S A Avdonin and S A Ivanov. *Families of exponentials. The method of moments in controllability problems for distributed parameter systems*. Cambridge University Press, Cambridge, 1995.
[36] A N Kolmogorov and S V Fomin. *Elements of the Theory of Functions and Functional Analysis*. Dover Publications Inc., Mineola, New York, 1999.
[37] S L Sobolev. *Partial Differential Equations of Mathematical Physics*. Dover Publications Inc., Mineola, New York, 1989.
[38] A N Tikhonov and A A Samarskii. *Equations of mathematical physics*. Dover Publications Inc., New York, 1990.
[39] A Quarteroni, R Sacco, and F Saleri. *Numerical Mathematics*. Springer-Verlag, New York, 2000.
[40] P Linz. *Analytical and Numerical Methods for Volterra Equations*. SIAM, Philadelphia, 1985.